

## Numerical Study of Thermosolutal Convection in Enclosures Used for Directional Solidification (Bridgman Cavity)

K. Achoubir<sup>1</sup>, R. Bennacer<sup>2</sup>, A. Cheddadi<sup>1</sup>, M. El Ganaoui<sup>3</sup> and E. Semma<sup>3,4</sup>

**Abstract:** The present work is devoted to the numerical investigation of the interaction between thermal and solutal convection in enclosures used for modeling directional solidification. The full transient Navier–Stokes, energy and species conservation equations are solved numerically by using finite volumes technique.

The effect of parameters governing the problem (namely the Rayleigh number,  $Ra$ , Lewis number,  $Le$ , and thermal to solutal ratio,  $N$ ) on the transition to oscillatory modes is studied for thermal and solutal buoyancy forces opposing each other.

In steady regimes and for moderate Lewis value ( $Le=10$ ), the flow structure and intensity are found to depend strongly on  $N$  ( $N$  is considered to vary between 0 and  $10^2$ ). For  $N = 1$ , the transition to oscillatory mode is studied as a function of the Lewis number. We show the existence of three distinct behaviours of the critical Rayleigh number. In the first domain ( $Le > 100$ ), the critical Rayleigh number tends to an asymptotic constant value. In the second domain (for intermediate  $4 < Le < 100$ ), the evolution of the critical Rayleigh number can be correlated by  $Ra_c \times Le^{-1/2} \propto 1$ . In the third domain ( $Le < 4$ ), where the scale for mass and energy diffusion are of the same order; a complex scenario caused by the strong competition between the solutal and the thermal forces is observed.

### Nomenclature

|        |   |
|--------|---|
| $C$    | dimensionless concentration                                     |
| $D$    | mass diffusivity  |
| $g$    | gravitational acceleration                                      |
| $H$    | height of the enclosure   |
| $k$    | thermal conductivity  |
| $Le$   | Lewis number, $=\alpha/D$                                       |
| $N$    | buoyancy ratio, $=\beta_C \Delta C' / \beta_T \Delta T'$        |
| $Nu$   | Nusselt number, see Eq (9)                                      |
| $Pr$   | Prandtl number, $=\nu/\alpha$                                   |
| $Ra$   | thermal Rayleigh number, $=g\beta_T \Delta T' H^3 / \nu \alpha$ |
| $Sh$   | Sherwood number, see Eq (9)                                     |
| $t$    | dimensionless time  |
| $T$    | dimensionless temperature                                       |
| $x, y$ | dimensionless coordinate system                                 |
| $u, v$ | dimensionless velocity terms                                    |

### Greek symbol

|          |                               |
|----------|-------------------------------|
| $\alpha$ | thermal diffusivity           |
| $\beta$  | expansion coefficient         |
| $\nu$    | kinematic viscosity of fluid  |
| $\rho$   | density of fluid              |
| $\psi$   | dimensionless stream function |

### Subscript

|     |             |
|-----|-------------|
| $c$ | critic      |
| $C$ | cold        |
| $H$ | hot         |
| max | maximum     |
| $S$ | solutal     |
| $T$ | temperature |
| 0   | reference   |

### Superscript

|     |                      |
|-----|----------------------|
| $'$ | dimensional variable |
|-----|----------------------|

<sup>1</sup> University Mohammed V, Ecole Mohammadia d'Ingénieur, Rabat, Maroc.

<sup>2</sup> University of Cergy Pontoise, LEEVAM, France

<sup>3</sup> Corresponding author. Email: ganaoui@unilim.fr. University of Limoges, SPCTS UMR 6638 CNRS, Limoges, France

<sup>4</sup> University Hassan 1<sup>er</sup>, FST de Settât, LAMS, Settât, Maroc.

## 1 Introduction

Applications arising in our epoch in electronics, telecommunications, photovoltaic, and space industry impose important challenges for scientific research in the field of material Sciences. With a few exceptions, most of the solid materials of interest in these fields undergo, at a crucial point of their history, a phase change transition from a liquid to a solid state. This transition is of great importance in material science and crystal growth processes. Control of fluid dynamic phenomena permits crystallisation of high quality pure crystals.

An issue of the *Comptes Rendus Mecanique* of the French Academy of Sciences on the field of 'Microgravity and Transfers', published by El Ganaoui and Prud'homme in 2004, has illustrated how performing experiments (in microgravity, in hyperbolic flights or in space vehicles) can significantly advance the understanding of liquid motion and of phenomena hidden under earth research. The use of numerical simulation can be regarded as an additional useful means for improving our understanding of the phase change process (Amberg and Shiomi 2005, Narski and Picasso, 2007, Sohail and Saghir 2006).

Numerical investigation of flow stability for a melt under directional solidification conditions enables one to identify the critical operating parameters for crystal growth. Hence there has been increased interest in the study of flows of liquid metals in cavities subjected to external temperature gradients. For practical applications, the dopant distribution is strongly linked to the fluid dynamic behaviour and takes advantage of stable solutions (Jaber and Saghir 2006, Sohail and Saghir 2006, Trivedia *et al.* 2001a). During solidification of binary alloys, the thermal and concentration buoyancy forces either aid or oppose each other, depending on the type of alloy, the phase diagram, the initial concentration of dopants, and the heating (or cooling) condition considered.

The classical directional solidification configuration (Bridgman) heated from the top, is more stable, the flow is weak and is mainly due to a two-dimensional temperature field which results

in a hot (less dense) stream of fluid descending towards the centre of the solid interface. For this classical case, two counter-rotating cells are formed. They accumulate solute near the interface (in hypoeutectic situation). Such solute accumulation can lead to morphological instabilities (Trivedia *et al.* 2001a, Trivedi, Liu, Mazumder and Simsek 2001b).

For the inverted Bridgman, flow results not only from the two-dimensional temperature field (discussed above) but also because of the classical Rayleigh-Benard convection (RB). The flow obtained for the same controlling parameters is much stronger. The stronger flow results in better species mixing (the flow intensity and the flow direction on the solid-liquid interface result on a more homogeneous species distribution).

Fluids heated from below exhibit very strong non-linear behaviour, which is of interest in many scientific fields and, in particular, in the electronic industry (interface shape is strongly affected by convection, (Brice 1976, McFadden and Coriel 1987)).

In general, enclosures heated from below are involved in several industrial processes (metallurgy, crystal growth, etc). The heat transfer in these configurations is extremely complex and is influenced by several factors such as the variation of the fluid thermophysical properties and thermal transfer modes (convection, radiation, conduction through the walls, etc).

Relatively simple geometries leading to two-dimensional models are commonly used for predictive numerical investigation of directional solidification configurations (Alexander *et al.* 1991, Lappa 2005, Impey *et al.* 1991, Ryskin *et al.* 2003).

In particular, square cavities with thermal boundary conditions close to those used in crystal growth with vertical Bridgman method have been widely studied in the literature (Calcagni, Marsili and Paroncini 2005, Kaenton *et al.* 2004, Larroudé *et al.* 1994, Punjabi, Muralidhar and Panigrahi 2006, Semma *et al.* 2006).

Larroudé *et al.* (1994) studied the oscillatory behaviour of the flow in a configuration heated from

below and subjected to a weak vertical translation. In their study, they considered predominance of the thermal convection on the solutal one. They identified symmetry breaking of the steady-state flow structure for low Rayleigh numbers and transition to oscillatory modes for moderate thermal Rayleigh numbers. The effect of a variety of parameters on heat and mass transfer in this kind of configurations (closed rectangular or cylindrical cavities) was the subject of subsequent analyses (Bennacer, Mohamad and Sezai 2001, Calcagni, Marsili and Paroncini 2005, Kaenton *et al.* 2004, Lan and Wang 2001, Punjabi, Muralidhar and Panigrahi 2006, Semma *et al.* 2006).

Several possible regimes of fluid convection have been summarized in a recent paper (Lappa 2007) dealing with secondary and oscillatory gravitational instabilities in canonical three dimensional models of crystal growth from melts (both RB systems and lateral heating with Hadley circulation have been considered).

Extensions to the presence of a solid/liquid interface starting from results for enclosures that were investigated without phase change are reported by El Ganaoui and Bontoux (1998) and El Ganaoui 2002. The authors showed important results for a better understanding of the transitional situations observed when considering the liquid/solid interface subject to deformation.

Other analyses have focused on aspects relative to the coupling between thermodiffusion and natural convection. The critical conditions corresponding to the onset of convection were determined by several authors for both horizontal and vertical rectangular enclosures (Bennacer *et al.* 2000, Ghorayeb, Khallouf and Mojtabi 1999, Bennacer *et al.* 1993, Mahidjiba *et al.* 2005, Sovran *et al.* 2001).

In general, two cases involving the thermosolutal convection can be distinguished according to whether the thermal and solutal buoyancy forces cooperate or oppose each other.

In the present study, we analyse the complex dynamic effects characterized by the appearance of various instability modes. The interaction between thermal and solutal convection, in partic-

ular, is examined in steady and unsteady conditions. Some useful correlations are derived.

## 2 Mathematical formulation and solution method

### 2.1 Problem formulation

The studied configuration, sketched in Figure 1 corresponds to a simplified variant of the Bridgman 3D furnace classical model. It consists of a square cavity heated from below and cooled from the top by maintaining the temperatures  $T'_H$  and  $T'_C$  of these surfaces constant. Constant concentrations:  $C'_0$  (at the top) and  $C'_1$  (at the bottom) are also considered leading to two characteristic differences  $\Delta T' = T'_H - T'_C$  and  $\Delta C' = C'_1 - C'_0$ . The cavity is filled with a binary fluid of a low Prandtl number (metallic melt with  $Pr=0.01$ ).

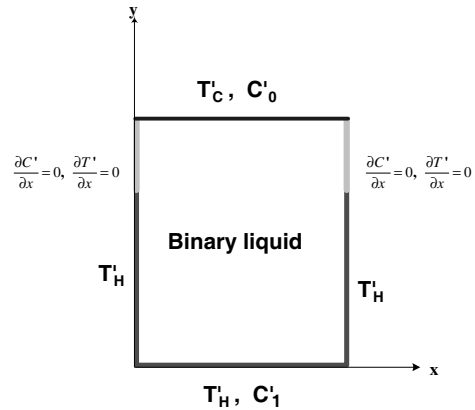


Figure 1: Sketch of the physical system

The fluid is Newtonian; the flow incompressible and radiative heat transfer is neglected. The Boussinesq approximation is assumed to be valid; the thermophysical properties are constant except the density in the buoyancy term (prime denotes dimensional variables):

$$\rho = \rho_0 [1 - \beta_T(T' - T'_0) + \beta_S(C' - C'_0)] \quad (1)$$

The dimensionless variables are defined as:

$$\begin{aligned} (x, y) &= (x'/H, y'/H), \quad t = \alpha t'/H^2, \\ (u, v) &= (u'H/\alpha, v'H/\alpha), \\ T &= (T' - T'_0)/\Delta T', \quad C = (C' - C'_0)/\Delta C' \end{aligned} \quad (2)$$

The motion of the fluid and transfers are governed by the Navier-Stokes equations coupled with energy and species equations which are expressed in dimensionless form as:

$$\frac{\partial u}{\partial x} + \frac{\partial v}{\partial y} = 0 \quad (3)$$

$$\frac{\partial u}{\partial t} + u \frac{\partial u}{\partial x} + v \frac{\partial u}{\partial y} = -\frac{\partial p}{\partial x} + Pr \nabla^2 u \quad (4)$$

$$\frac{\partial v}{\partial t} + u \frac{\partial v}{\partial x} + v \frac{\partial v}{\partial y} = -\frac{\partial p}{\partial y} + Pr \nabla^2 v + Ra_T Pr (T - NC) \quad (5)$$

$$\frac{\partial T}{\partial t} + u \frac{\partial T}{\partial x} + v \frac{\partial T}{\partial y} = \nabla^2 T \quad (6)$$

$$\frac{\partial C}{\partial t} + u \frac{\partial C}{\partial x} + v \frac{\partial C}{\partial y} = \frac{1}{Le} \nabla^2 C \quad (7)$$

The problem is governed by four dimensionless numbers: the thermal Rayleigh number,  $Ra_T = g\beta_T \Delta T' H^3 / \nu \alpha$ , the Prandtl number,  $Pr = \nu / \alpha$ , the Lewis number,  $Le = \alpha / D$ , and the buoyancy ratio  $N = \beta_S \Delta C' / \beta_T \Delta T'$ .

When the two buoyancy forces related to temperature and concentration act in the opposite direction; the buoyancy ratio  $N$  is defined positive ( $N > 0$ ). The dynamic boundary conditions are no slip on the solid-liquid interfaces. The temperature and concentration boundary conditions are:

$$T(0, y) = T(1, y) = 1 \text{ for } y \in [0, 0.75]$$

$$T(x, 1) = 0, \quad T(x, 0) = 1 \text{ for } x \in [0, 1]$$

$$\left. \frac{\partial T(x, y)}{\partial x} \right|_{x=0} = \left. \frac{\partial T(x, y)}{\partial x} \right|_{x=1} = 0 \text{ for } y \in [0.75, 1] \quad (8)$$

$$C(x, 0) = 1 \quad \text{and} \quad C(x, 1) = 0$$

$$\left. \frac{\partial C(x, y)}{\partial x} \right|_{x=0} = \left. \frac{\partial C(x, y)}{\partial x} \right|_{x=1} = 0$$

Nusselt and Sherwood numbers characterizing, respectively, the dimensionless heat and mass transfer are defined as:

$$Nu = \int_{x=0}^{x=1} \left. \frac{\partial T}{\partial y} \right|_{y=1} dx \quad \text{and} \quad Sh = \int_{x=0}^{x=1} \left. \frac{\partial C}{\partial y} \right|_{y=1} dx \quad (9)$$

## 2.2 Numerical approximations and validation

For numerical approximations of the considered problem a finite volume method has been used (Patankar, 1980). The conductive terms have been discretized with a central scheme and the convective terms by using a third order QUICK scheme subjected to a flux limiter developed by Leonard (Leonard 1991, Leonard 1979). To resolve the velocity - pressure coupling, the SIMPLEC algorithm has been used (Van Doormaal and Raithby 1984). The temporal discretization is done using a second order Euler scheme. Extensive validation of the performance of the present code with and without phase change has been done elsewhere (Semma *et al.* 2005).

The numerical method has been validated by comparison with the results of Bergman and Hyun (1996). The configuration considered is a laterally heated square cavity. The left and right walls are respectively maintained with uniform concentrations ( $C' = 1$ , rich in *Sn*) and ( $C' = 0$ , rich in *Pb*). Bergman and Hyun carried out simulations by a spectral method and obtained solutions of high accuracy in a broad range of thermal and solutal Rayleigh numbers. We illustrate here the comparison with the case corresponding to  $Ra = 100$  and  $N = 10$ . At small times, and because  $Le = 7500$ , the thermal buoyancy forces dominate and give rise to a one convection cell occupying the whole domain. In the same way, two solutal boundary layers are developed near the vertical walls giving place to secondary cells turning in the opposite direction. These cells grow with time reducing thus the size of the thermal cell. This can be also illustrated by the significant decrease of the stream function value from 5.00 to 0.339 for  $t = 0.3$  and  $t = 3.15$ , respectively (see Figure 2). Computations give a good agreement with the results of Bergman and Hyan showing the reliability of the present method in describing with a good accuracy thermo-solutal competition.

A mesh refinement study was carried out from  $32^2$  to  $128^2$  grid points and showed that spatial resolution  $64^2$  and time step  $\Delta t = 5 \times 10^{-4}$  allow an accurate description of the thermosolutal convection phenomena within the cavity. Convergence is assumed for a maximum value of the relative

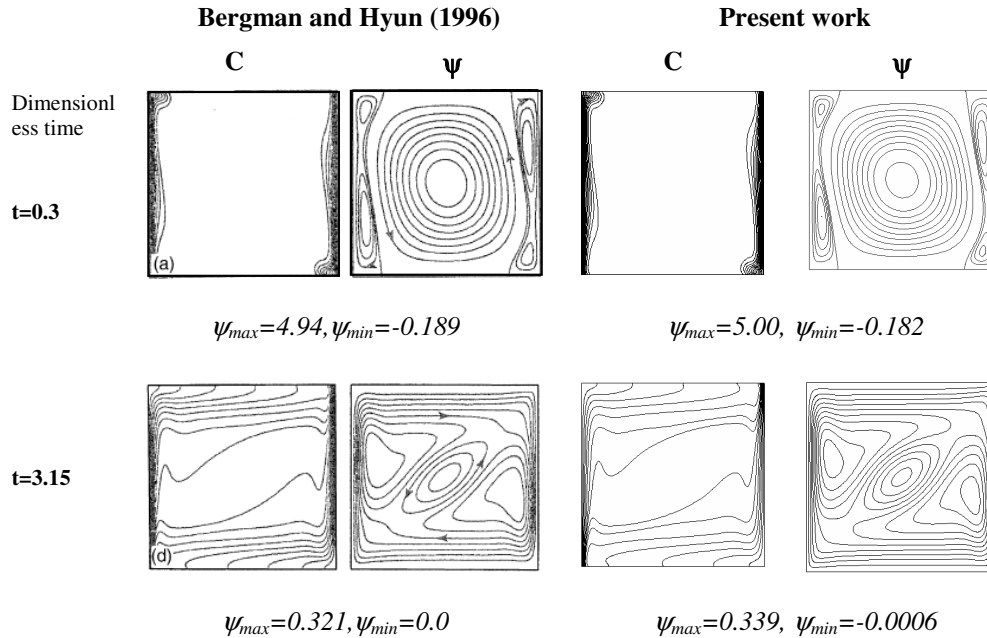


Figure 2: Comparison between present results and Bergman and Hyun (1996) calculations. Distribution of the concentration and streamlines with extreme stream function values ( $Ra = 100$  and  $N = 10$ )

error of principal variables lower than  $10^{-6}$ .

### 3 Results and discussion

Without solutal convection ( $N = 0$ ), the Bridgman vertical cavity heated from below is characterized by the appearance of unstable modes for relatively low values of thermal Rayleigh number (Larroudé *et al.* 1994). The bifurcation diagram shows the existence of a narrow stable branch located in the interval  $[0-17500]$  with a transition from a stationary bi-cellular flow regime to an asymmetrical mono-cellular one at  $Ra = 3500$  (Semma *et al.* 2006).

We underline that the symmetry breaking observed in 2D is more complex under a 3D approach. The pure thermal 3D case was studied by Bennacer, El Ganaoui and Leonardi (2006), where multiple solutions were possible in the cavity and a fully 3D flow was observed at a critical Rayleigh number lower than the 2D estimated threshold.

It is known that 2D oscillatory flow starts with a mono-periodical mode with predominance of only one flow cell before forking towards a quasi periodic regime at double period and finally to

non periodic behaviour for higher  $Ra$ .

In order to quantify the relative solutal effect on the thermal one described above, we will discuss first the steady state regimes in the range of  $N$  from the pure thermal convection condition ( $N = 0$ ) to the case of dominant solutal forces ( $N \gg 1$ ).

The second part is devoted to the unsteady regime, where the buoyancy forces increase and the Lewis number exhibits a threshold above which oscillatory solutions are obtained.

#### 3.1 Steady regime

A moderate Lewis number ( $Le = 10$ ) is used to analyse the thermosolutal stationary regime. We consider two Rayleigh number values ( $Ra = 10^3$  and  $10^4$ ) corresponding to the two different steady flow structures found in the thermal configuration ( $N = 0$ ). Such flows are characterized by either a monocellular flow or two contra-rotating cells (cf. Figure 3). The two possible solutions are of different intensity with weaker flow intensity in the counter-rotating case. Such a regime corresponds to a thermal field mainly conductive (see Figure 4) and the related flow is mainly due to the imposed

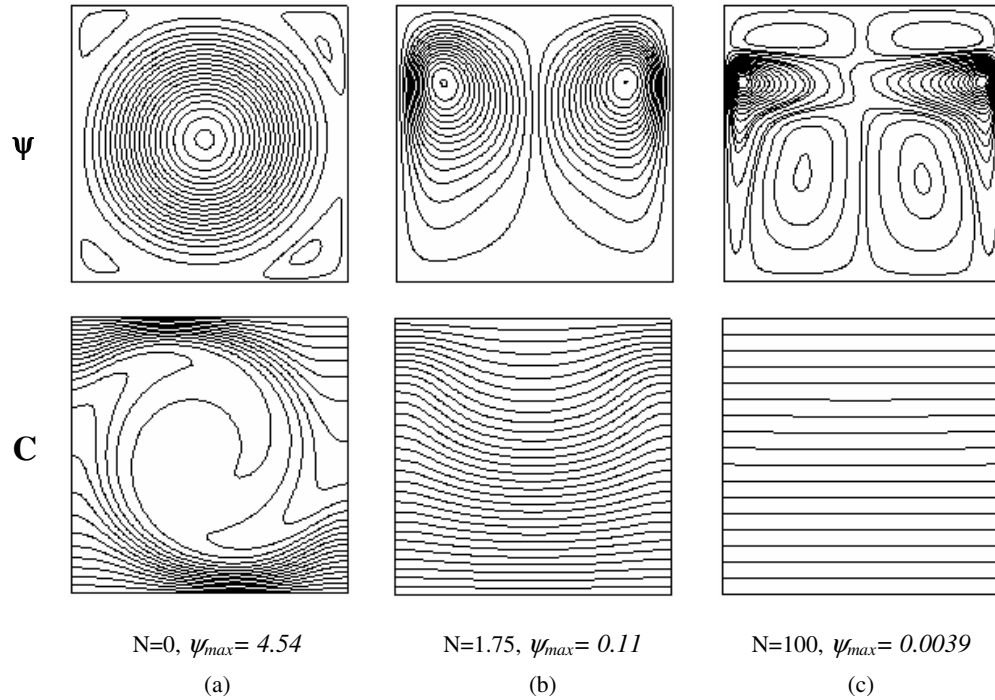


Figure 3: Various types of stationary solutions, ( $Ra = 10^4$ ,  $Pr = 0.01$ ,  $Le = 10$ )

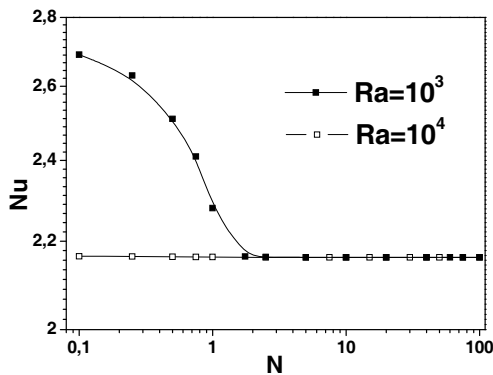


Figure 4: Variation of Nusselt number according to  $N$  ( $Le = 10$ ,  $Pr = 0.01$ )

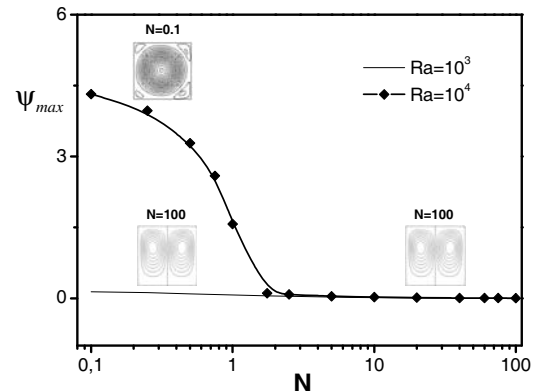


Figure 5: Variation of the maximum of the flow intensity according to  $N$  ( $Le = 10$ ,  $Pr = 0.01$ )

horizontal temperature gradient resulting from the lateral heating. As explained before, the monocellular flow case corresponds to a set of convective roll above a critical  $Ra$  value. The vortex rotation can be either clockwise or counterclockwise.

For illustrating the thermosolutal competition, we consider a large range of  $N$  ( $0 \leq N \leq 100$ ). The flow intensity versus  $N$  is represented in Figure 5 for the two considered  $Ra$  numbers of  $10^3$  and  $10^4$ . For the low  $N$  values ( $N \ll 1$ ), the solutal

buoyancy forces are not sufficient to counterbalance the thermal buoyancy forces. The obtained mass transfer (Figure 6) is a weak function of  $N$ . The mass transfer is more intense than the heat transfer (compare Figures 4 and 6) because it is more sensitive to fluid motion due to the large Lewis number value of,  $Le = 10$ . The chosen  $Le$  number corresponds to a case of weak coupling of the thermal and dynamic fields.

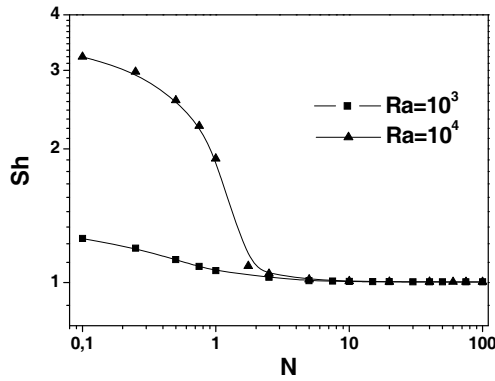


Figure 6: Variation of Sherwood number according to  $N$  ( $Le = 10$ ,  $Pr = 0.01$ )

The mass transfer for  $Ra = 10^3$  shows a fall of about 20% for  $N$  varying from 0 to 1. In the case of solutal effect dominant, *i.e.* important  $N$  values, the flow intensity, heat and mass transfer decrease and tend to the diffusive regime with a non significant remaining flow. Such behaviour is due to the stabilizing applied solutal condition. In the diffusive regime the obtained  $Nu$  is two times  $Sh$  (Figure 4 and 6) and such result is a consequence of the applied boundary condition for which a constant temperature is applied on both vertical and horizontal surfaces. Interestingly, the 2D thermal boundary conditions induce two secondary cells located near the cold wall. These cells having weak intensity affect slightly the asymptotic heat and mass diffusive transfer.

For  $Ra = 10^4$  and  $N = 0$ , the flow is characterized by one flow cell (clockwise or counter-clockwise) occupying the whole domain. When  $N$  increases from 0 to 1, the flow intensity decreases nearly by 50%, indicating the development of the stabilizing effect exerted by the solutal convection (Figures 5 and 6) from the immediate vicinity of the lower surface.

As illustrated before, for low  $N$  values, the flow structure is monocellular (Figure 3-a) or bicellular (Figure 3-b). The related solutal field illustrates the mixing ability of such flows and acts as passive scalar transport. When  $N$  increases, the size of the secondary cells observed in monocellular case localised at the cavity corners increases and extends until the flow becomes symmetrical

(with two cells). When  $N$  reaches a large value a no-flow zone appears, and this zone height increases with  $N$  (figure 3-c). Such stable situation is possible for  $Ra$  value lower than the critical  $Ra$  number (Bahloul *et al.* 2004, Mahidjiba, Bennacer and Vasseur 2003). The size of the remaining convective cell ( $\zeta$ ) was evaluated from the scale analysis (Bennacer, Mohamad and Akrou 2001) to be:

$$49\zeta(1 - \zeta)^{1/2} \approx N(LeA)^{-1/2}Ra^{-1/2} \quad (10)$$

### 3.2 Unsteady regime

The beginning of the unsteady flow depends on the interplay of the parameters governing the problem and is very sensitive to  $Le$  and  $N$ . As discussed before, in steady state regimes, the flow falls from strong to weak intensity. In such a situation, the change of the flow structure and of the heat and mass transfer observed around  $N \sim 1$  can be explained by the equilibrium between the two types of counteracting buoyancy forces. Thus, in the present section, we consider  $N = 1$ , and we investigate the critical value of Rayleigh number.

Typical mass transfer and flow pattern versus time are represented on figure 7 for  $Ra = 10^3$ ,  $10^4$  and  $1.6 \times 10^4$  corresponding to diffusive, convective and oscillatory regimes, respectively. The flow intensity, as expected, increases with  $Ra$  and exhibits oscillation for the case considered here ( $A = 1$ ,  $Le = 10$  and  $Pr = 0.01$ ).

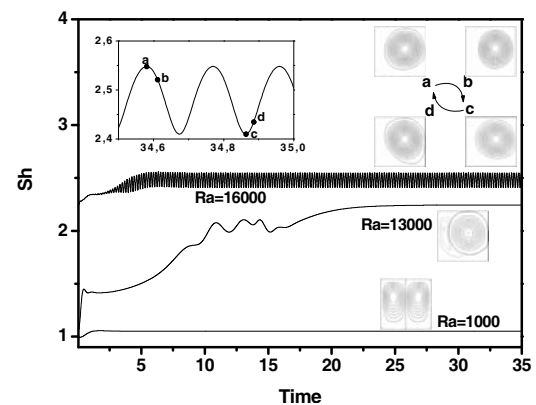


Figure 7: Sherwood number versus time for different  $Ra$

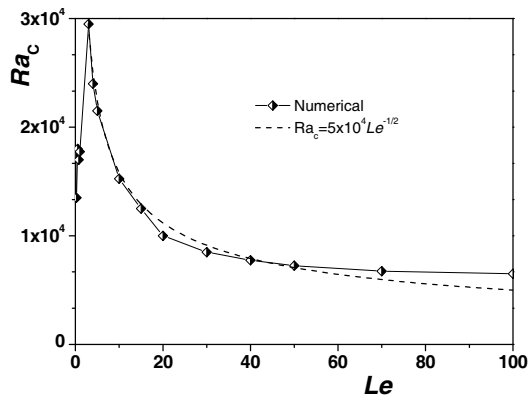


Figure 8: Variation of the critical thermal Rayleigh according to the Lewis number ( $N = 1$ ,  $Pr = 0.01$ )

The oscillatory regime is a consequence of thermal and solutal time diffusion characteristics and the competition is on the corresponding different boundary layer scales. The  $Ra$  threshold transition from steady state to oscillatory behaviour depends on the relative length scales controlled by  $Le$ . Figure 8 shows the evolution of such critical  $Ra_c$  versus  $Le$ . Four distinct regimes appear in figure 8:

1. For the low values of  $Le$  ( $<0.2$ ), when the Rayleigh number exceeds the critical value, the flow becomes oscillatory (periodic with a frequency of about 6). Such asymptotic tendency corresponds to a situation where the solutal field is mainly diffusive and the convective flow is strongly coupled to the thermal field.
2. For  $Le$  between 0.1 and 3, the mono-cellular stationary regime disappears and the transition to the oscillatory mode is due to the competition of two basic flow cells. The oscillation frequency is very small (about 0.1 for  $Le = 0.25$ ). The absence of mono-cellular flow mode for this range of Lewis number can be explained by the stabilizing effect of the solutal forces preventing the bifurcation towards convective modes.
3. For  $Le$  higher than 4 and less than 100, solutal composition distribution becomes sensitive to the flow regime. The oscillatory

regime is characterized by the dominance of only one flow cell. Four secondary cells take place in the four corners in the cavity. Evolution of the critical Rayleigh number in this range of  $Le$  can be correlated by:

$$Ra_c \propto Le^{-1/2} \quad (11)$$

Note that in a similar configuration with a cross thermal gradient condition (Bennacer, Mohamad and Akrouf 2001), a subcritical  $Ra_c$  value was also identified to vary as  $Le^{-1/2}$ .

4. For  $Le$  higher than 100, a fourth tendency seems to appear where the critical  $Ra$  number becomes constant. The corresponding very thin solutal boundary layer has relatively no significant effect on the global flow and the obtained oscillation behavior tends to be controlled by the thermal field.

#### 4 Conclusion

The present work has considered the investigation of a low Prandtl number material in a typical configuration for directional solidification. The interaction between thermal and solutal convection has been examined in steady and unsteady regimes under the conditions of  $Pr=0.01$  and  $A = 1.0$ .

The flow structure has shown the existence of mono cellular and bi-cellular flows according to the parameter  $N$ .

The mass transfer is more intense than the heat transfer because it is more sensitive to the flow due to the considered Lewis number. The chosen  $Le$  number (of 10) corresponds, in fact, to weak coupling of the thermal and hydrodynamic fields.

The transition to unsteady regimes has been also considered. Four cases for the dependence of the critical Rayleigh number on  $Le$  have been identified depending on the solutal diffusive mode in the cavity. These cases depend also on the degree of coupling of heat and mass transfer with the fluid flow. An asymptotic behaviour has been observed for high values of  $Le$ .

**Acknowledgement:** E. Semma thanks the University of Limoges of visiting position during

2006/2007 when a part of this work has been achieved. Authors also thank Prof. J. Masliyah and A. A. Mohamad for fruitful discussion during his visit to the University of Limoges.

## References

- Alexander J.; Amiroudine S.; Ouazzani J.; Rozenberger F.** (1991): Analysis of the low gravity tolerance of Bridgman-Stockbarger crystal growth II. Transient and periodic accelerations, *J. Crystal Growth*, vol. 113, pp. 21-38.
- Amberg G.; Shiomi J.** (2005): Thermocapillary flow and phase change in some widespread materials processes, *FDMP: Fluid Dynamics & Materials Processing*, vol. 1, no. 1, pp. 81-95.
- Bahloul A.; Kalla L.; Bennacer R.; Beji H.; Vasseur P.** (2004): Natural convection in a vertical porous slot heated from below and with horizontal concentration gradients, *International Journal of Thermal Sciences*, vol. 43, no. 7, pp. 653-663.
- Bennacer R.; Beji H.; Duval R.; Vasseur P.** (2000): The Brinkman Model For Thermosolutal Convection In A Vertical Annular Porous Layer, *International Communication Of Heat And Mass Transfert*, vol. 27, no. 1, 69-80.
- Bennacer R.; El Ganaoui M.; Leonardi E.** (2006): Vertical Bridgman Configuration Heated From Below: 3d Bifurcation And Stability Analysis, *Applied Mathematical Modelling*, vol. 30, no. 11, pp. 1249-1261.
- Bennacer R.; Mohamad A.A.; Akrouf D.** (2001): Transient natural convection in an enclosure with horizontal temperature and vertical solutal gradients, *Int. J. Therm. Sci.*, vol. 40, pp. 899-910.
- Bennacer R.; Mohamad A.A.; Sezai I.** (2001): Transient natural convection in air-filled cubical cavity: Validation Exercise, *CHT'01 Advances in Computational Heat Transfer II*, G. de Vahl Davis and E. Leonardi (eds), Begell House Inc., New York, pp. 1385-1390.
- Bennacer R.; Sun, L.Y.; Toguyeni Y.; Benard C.** (1993): Structure d'écoulement et transfert de chaleur par convection naturelle au voisinage du maximum de densité, *International Journal of Heat and Mass Transfer*, vol. 36, no. 13, pp. 3329-3342.
- Bergman T.L.; Hyun M.T.** (1996): Simulation of two-dimensional thermosolutal convection in liquid metals induced by horizontal temperature and species gradients, *Int. J. Heat Mass Transfer*, vol. 39, no. 14, pp. 2883-2894.
- Brice J.C.** (1976): *The growth of crystals from liquids*. North-Hollands, New York.
- Calcagni B.; Marsili F.; Paroncini M.** (2005): Natural convective heat transfer in square enclosures heated from below, *Applied Thermal Engineering*, vol. 25, pp. 2522-2531.
- El Ganaoui M.; Bontoux P.** (1998): An homogenisation method for solid-liquid phase change during directional solidification, ASME, H.T.D., *Numerical and Experimental Methods in Heat Transfer*, éd. R.A. Nelson, T. Chopin, S.T. Thynell, vol. 361 no. 5, 453-469.
- El Ganaoui M.** (2002): Computational modeling of heat mass and solute transport in solid/liquid transition systems on earth and on microgravity environment. *Mecanica Computational*, vol XXI, ISSN 1666-6070, Eds. S.R. Idelsohn, V. Sonzogni, A. Cardona, p. 2587-2592.
- El Ganaoui M., Prud'homme R.** (Ed) (2004): Microgravity and transfers, *spécial issue Comptes Rendus Mécanique*, vol. 332, no. 5-6.
- Ghorayeb C.K.; Khallouf, Mojtabi A.** (1999): Onset of oscillatory flows in double diffusive convection, *Int. J. Heat Mass Transfer*, vol. 42, pp. 629-643.
- Jaber T.J.; Saghir M.Z.** (2006): The Effect of Rotating Magnetic Fields on the Growth of SiGe Using the Traveling Solvent Method, *FDMP: Fluid Dynamics & Materials Processing*, Vol. 2, No.3, pp. 175-190.
- Joly F.; Vasseur P.; Labrosse G.** (2001): Soret instability in a vertical Brinkman porous enclosure, *Numerical Heat Transfer, Part A*, vol. 39, pp. 339-359.
- Kaenton J.; Timchenko V.; Semma E.A.; Leonardi E.; El Ganaoui M.; de Vahl Davis G.** (2004): Effects of anisotropy and solid/liquid

thermal conductivity ratio on flow instabilities during inverted Bridgman growth. *Int. J. Heat and Mass Transfer*, vol. 47, no. 14-16, pp. 3403-3413.

**Lan C.W.; Wang C.H.** (2001): Three-dimensional bifurcations of a two phases Rayleigh-Benard problem in a cylinder, *Int. J. Heat and Mass Transfer*, 44, pp. 1823-1836.

**Lappa M.** (2005): On the nature and structure of possible three-dimensional steady flows in closed and open parallelepipedic and cubical containers under different heating conditions and driving forces, *FDMP: Fluid Dynamics & Materials Processing*, vol. 1, no. 1, pp. 1-19.

**Lappa M.** (2007): Secondary and oscillatory gravitational instabilities in canonical three-dimensional models of crystal growth from the melt. Part 2: Lateral Heating and the Hadley Circulation, *special issue comptes rendues de mécanique*, Editors M. El Ganaoui, R. Prud'homme, R. Bennacer, 261-268.

**Larroudé P.; Ouazzani J.; Alexander J.I.D.; Bontoux P.** (1994): Symmetry breaking transition and oscillatory flows in a 2D directional solidification model, *Eur. J. Mech, B/Fluids*, vol. 13, no. 3, pp. 353-381.

**Leonard B.P.** (1979): A stable and accurate convective modeling procedure based on quadratic upstream interpolation, *Comput. Methods Appl. Mech. Eng.*, vol. 19, pp. 59-98.

**Leonard B.P.** (1991): The ultimate conservative difference scheme applied to unsteady one-dimensional advection, *Comp. Methods in App. Mech. And Engineering*, vol. 88, pp. 17-74.

**Impey, M.D.; Riley, D.S.; Wheeler A.A.; Winters K.H.** (1991): Bifurcation analysis of solutal convection during directional solidification. *Phys. Fluids A*, vol. 3, pp. 535.

**Mahidjiba A.; Bennacer R.; Vasseur P.** (2003): Effect of the boundary conditions on convection in a horizontal fluid layer with the Soret contribution, *Acta Mechanica*, vol. 160, pp. 161-177.

**Mahidjiba A.; Bennacer R.; Vasseur P.** (2005): Flows in a fluid layer induced by the combined action of a shear stress and the Soret effect, *Int. J. Heat Mass Transfer*, vol. 49, pp. 1403-1411.

**McFadden B.; Coriell S.R.** (1987): Thermosolutal convection during directional solidification. II. Flow transitions. *Phys. Fluids*, vol. 30, pp. 659-671.

**Narski J.; Picasso M.** (2007): Adaptive 3D finite elements with high aspect ratio for dendritic growth of a binary alloy including fluid flow induced by shrinkage, *FDMP: Fluid Dynamics & Materials Processing*, vol. 3, no. 1, pp. 49-64.

**Patankar S.V.** (1980): *Numerical heat transfer and fluid flow*, McGraw-Hill.

**Punjabi S.; Muralidhar K.; Panigrahi P.K.** (2006): Influence of Layer Height on Thermal Buoyancy Convection in A System with Two Superposed Fluids Confined in A Parallelepipedic Cavity, *FDMP: Fluid Dynamics & Materials Processing*, vol. 2, no. 2, pp. 95-106.

**Ryskin A.; Müller H.W.; Pleiner H.** (2003): Thermal convection in binary fluid mixtures with weak concentration diffusivity, but strong solutal buoyancy forces, *Physical Review E*, vol. 67, pp. 1-8.

**Semma A.; El Ganaoui M.; Cheddadi A.; Farchi A.** (2005): *High Order Finite volumes scheme for phase change problems*, Finite Volume for complex Applications IV, Hermes Science publishing, Eds. F. Benkhaldoun, D. Ouazzar, S. Raghay, pp. 493-503.

**Semma E.A.; El Ganaoui M.; Timchenko V.; Leonardi E.** (2006): Some Thermal Modulation Effects on Directional Solidification, *FDMP: Fluid Dynamics & Materials Processing*, vol. 2, no.3, pp. 191-202.

**Sohail M.; Saghir M.Z.** (2006): Three-Dimensional Modeling of the Effects of Misalignment on the Growth of Ge<sub>1-x</sub>Si<sub>x</sub> by The Traveling Solvent Method, *FDMP: Fluid Dynamics & Materials Processing*, vol. 2, no. 2, pp. 127-140.

**Sovran O.; Charrier-Mojtabi M.C.; Mojtabi A.** (2001): Naissance de la convection thermosolutale en couche poreuse infinie avec effet Soret, *C. R. Acad. Sci. Paris*, vol. 329, pp. 287-293.

**Trivedi R.; Liu S.; Mazumder P.; Simsek E.** (2001b): Microstructure development in the directionally solidified Al-4.0 wt% Cu alloy sys-

tem, *Science and Technology of Advanced Materials*, vol. 2, no. 1, pp. 309-320.

**Trivedi R.; Miyaharab H.; Mazumderc P.; Simseka E.; Tewarid S.N.** (2001a): solidification microstructures in diffusive and convective regimes, *J. Crystal Growth*, vol. 222, pp. 365-379.

**Van Doormaal J.P.; Raithby G.D.** (1984): Enhancements of the SIMPLE method for predicting incompressible fluid flows. *Numerical Heat Transfer*, vol. 7, pp. 147-163.

